



OPEN

## Ribonuclease-1 treatment after traumatic brain injury preserves blood–brain barrier integrity and delays secondary brain damage in mice

Tobias J. Krämer<sup>1,8</sup>, Per Hübener<sup>1</sup>, Bruno Pöttker<sup>1</sup>, Christina Gölz<sup>1</sup>, Axel Neulen<sup>2</sup>, Tobias Pantel<sup>2</sup>, Hermann Goetz<sup>3</sup>, Katharina Ritter<sup>1</sup>, Michael K. E. Schäfer<sup>1,4,5,6</sup> & Serge C. Thal<sup>1,4,6,7</sup>✉

Traumatic brain injury (TBI) involves primary mechanical damage and delayed secondary damage caused by vascular dysfunction and neuroinflammation. Intracellular components released into the parenchyma and systemic circulation, termed danger-associated molecular patterns (DAMPs), are major drivers of vascular dysfunction and neuroinflammation. These DAMPs include cell-free RNAs (cfRNAs), which damage the blood–brain barrier (BBB), thereby promoting edema, procoagulatory processes, and infiltration of inflammatory cells. We tested the hypothesis that intraperitoneal injection of Ribonuclease-1 (RNase1, two doses of 20, 60, or 180 µg/kg) at 30 min and 12 h after controlled-cortical-impact (CCI) can reduce secondary lesion expansion compared to vehicle treatment 24 h and 120 h post-CCI. The lowest total dose (40 µg/kg) was most effective at reducing lesion volume (–31% RNase 40 µg/kg vs. vehicle), brain water accumulation (–5.5%), and loss of BBB integrity (–21.6%) at 24 h post-CCI. RNase1 also reduced perilesional leukocyte recruitment (–53.3%) and microglial activation (–18.3%) at 120 h post-CCI, but there was no difference in lesion volume at this time and no functional benefit. Treatment with RNase1 in the early phase following TBI stabilizes the BBB and impedes leukocyte immigration, thereby suppressing neuroinflammation. RNase1-treatment may be a novel approach to delay brain injury to extend the window for treatment opportunities after TBI.

Mechanical stress to brain tissue induces necrosis and apoptosis (termed primary injury), resulting in the release of cellular contents into the brain parenchyma and blood circulation<sup>1</sup>. Some intracellular biomolecules, including cell-free/extracellular ribonucleic acids (cfRNAs/eRNAs) act as damage-associated molecular patterns (DAMP) with potent pro-inflammatory activity<sup>2</sup>. cfRNA is present in plasma as nucleotide chains that are not bound to other molecules, is bound to proteins, or is stored in extracellular membrane vesicles<sup>3,4</sup>. In the latter two cases, cfRNA is protected from degradation by RNases<sup>5</sup>. These cfRNAs are abundant in the extracellular milieu after traumatic brain injury (TBI)<sup>2</sup>, where they promote vascular endothelial growth factor (VEGF) activation and ensuing disruption of the blood–brain barrier (BBB), leading to edema and immune cell infiltration<sup>6</sup>. These delayed processes are central drivers of the more expansive secondary damage following local TBI<sup>7–9</sup>. Cell-free

<sup>1</sup>Department of Anesthesiology, University Medical Center of Johannes Gutenberg University, Langenbeckstrasse 1, 55131 Mainz, Germany. <sup>2</sup>Department of Neurosurgery, University Medical Center of Johannes Gutenberg University, Langenbeckstrasse 1, 55131 Mainz, Germany. <sup>3</sup>Cell Biology Unit, University Medical Center of Johannes Gutenberg University, Langenbeckstrasse 1, 55131 Mainz, Germany. <sup>4</sup>Focus Program Translational Neurosciences, University Medical Center of Johannes Gutenberg University, Langenbeckstrasse 1, 55131 Mainz, Germany. <sup>5</sup>Research Center for Immunotherapy, University Medical Center of Johannes Gutenberg University, Langenbeckstrasse 1, 55131 Mainz, Germany. <sup>6</sup>Center for Molecular Surgical Research, University Medical Center of Johannes Gutenberg University, Langenbeckstrasse 1, 55131 Mainz, Germany. <sup>7</sup>Department of Anesthesiology, Helios University Hospital Wuppertal, University Witten/Herdecke, Heusnerstrasse 40, 42283 Wuppertal, Germany. <sup>8</sup>Faculty of Health, University Witten/Herdecke, Witten, Germany. ✉email: serge@thal.de

RNA has been reported to promote intercellular adhesion molecule-1 (ICAM-1)-dependent endothelial adhesion and extravasation of leukocytes<sup>10</sup>. Further, sequence-specific cfRNA binding to toll-like receptors (TLRs, such as TLR7, 8, and 12) activates NF- $\kappa$ B pathway signaling and upregulates production of the pro-inflammatory cytokine tumor necrosis factor- $\alpha$  (TNF- $\alpha$ ) by macrophages and microglia<sup>11,12</sup>. Extracellular RNAs have also been shown to increase expression of cytokines by macrophages via TLR3<sup>13,14</sup>, enhance interferon- $\gamma$  expression by astrocytes and microglia<sup>15,16</sup>, support the maturation of dendritic cells<sup>17</sup>, and exacerbate apoptosis via TLR3<sup>18,19</sup>. Several animal studies that have examined the efficacy of immunomodulatory agents in improving outcomes after TBI have yielded positive results<sup>20,21</sup>. Thus, elimination of cfRNAs at the site of injury or in the circulation could prevent secondary injury after TBI by stabilizing the BBB and promoting immunosuppression<sup>22,23</sup>.

The half-life of circulating cfRNA is dependent on plasma ribonuclease levels<sup>24</sup>. Ribonuclease-1 (RNase1) is a member of the RNase-A superfamily expressed in exocrine pancreas<sup>25</sup>, brain<sup>26</sup>, and in vascular endothelial cells<sup>27,28</sup>. The present study was designed to examine if RNase1 treatment post-TBI reduces brain edema, preserves BBB integrity, reduces brain lesion size, quells the neuroinflammatory response, and (or) improves functional outcome at 24 and 120 h after controlled-cortical-impact (CCI) in mice.

## Results

Animals were randomly assigned to receive a low-dose of RNase1 (LD:  $2 \times 20 \mu\text{g}/\text{kg}$ ,  $n = 10$ ), an intermediate-dose of RNase1 (MD:  $2 \times 60 \mu\text{g}/\text{kg}$ ,  $n = 10$ ), a high-dose of RNase1 (HD:  $2 \times 180 \mu\text{g}/\text{kg}$ ,  $n = 10$ ), or vehicle ( $2 \times 500 \mu\text{L}$  NaCl 0.9%,  $n = 10$ ) by i.p. injection 30 min and 12 h post-CCI. Contusion volume increase by 60% within 24 h, indicating induction of secondary injury<sup>29,30</sup>. However, all RNase1 doses significantly reduced lesion volume compared to vehicle treatment (vehicle:  $22.6 \pm 2.7 \text{ mm}^3$ ; LD:  $14.1 \pm 2.2 \text{ mm}^3$ ; MD:  $16.3 \pm 2.9 \text{ mm}^3$ ; HD:  $15.6 \pm 2.4 \text{ mm}^3$ ; all  $p < 0.001$ ; Fig. 1A). Lesion volumes continued to increase in all groups up to 120 h post-CCI and stabilized thereafter. Thus, post-CCI treatment with RNase1 can delay but not completely prevent brain damage (vehicle:  $27.3 \pm 4.4 \text{ mm}^3$ ; LD:  $28.1 \pm 2.4 \text{ mm}^3$ ; Fig. 1B). Neurofunctional impairment was assessed by a deficit score ranging from 0 (no motor deficits) to 15 (severe impairment) according to the criteria of Timaru-Kast and colleagues<sup>34</sup>. There were no significant differences in scores among groups at 24 h post-CCI, although low-dose RNase1 treatment resulted in an overall reduction compared to vehicle ( $4.5 \pm 1.3$  vs.  $5.9 \pm 1.9$ ,  $p = 0.0658$ ) (Fig. 1C). Prior to trauma, the animals averaged 61.3 s in the acceleration task on the rotarod and up to an average speed of 5.7 rounds per minute. There were no differences in motor function as assessed in the rotarod task at 120 h post-CCI. (Fig. 1D).

To examine if RNase1 treatment suppresses neuroinflammation, mRNA expression levels of interleukin (IL)-1 $\beta$  (Fig. 2A) and IL-6 (Fig. 2B) were determined in brain samples from the lesioned (ipsilateral) hemisphere by qPCR at 24 h post-CCI. No differences were present between RNase1 or vehicle treated animals. In addition, the number of activated microglia in the ipsilateral hemisphere as indicated by Iba-1 immunostaining was elevated in all treatment groups compared to the corresponding contralateral hemisphere and did not differ among groups at 24 h post-CCI (Fig. 2C). In contrast, cerebral inflammation was enhanced in the ipsilateral hemisphere at 120 h post-CCI, and both the numbers of Iba-1 + and CD45 + cells were significantly reduced by RNase1 treatment (Iba-1 +,  $p = 0.029$ ; CD45 +,  $p = 0.01$ ) (Fig. 2D,E).

In a separate set of animals, brain water content and BBB permeability were compared between brain injured animals receiving vehicle or LD RNase1 treatment and sham operated animals with LD RNase1 treatment ( $n = 10$  mice per group). LD was selected as the most effective dose from the previous experiments. First, the influence of LD RNase1 on post-CCI brain edema was examined by measuring the brain water content by vacuum drying. Treatment with RNase1 significantly reduced post-CCI brain water content from  $81.6\% \pm 2.3\%$  (contralateral:  $74.9\% \pm 1.1\%$ ) to  $77.1\% \pm 2.0\%$ ,  $p = 0.0027$  (contralateral:  $72.1\% \pm 2.3\%$ ), suggesting prevention of post-CCI edema. However, post-CCI water content was still significantly higher than contralateral or in the sham group (ipsilateral:  $72.3\% \pm 2.3\%$ ;  $p < 0.001$ ; contralateral:  $73.6\% \pm 2.0$ ; Fig. 3A), indicating only partial efficacy. To determine if LD RNase1 treatment also stabilizes BBB integrity, IgG extravasation was quantified as a surrogate parameter of functional integrity of the blood–brain barrier (BBB). These measurements revealed a 2–threefold higher signal in post-CCI tissue compared to sham operated animals (Fig. 3B) and a significant reduction by RNase1 treatment (40% lower IgG extravasation,  $p = 0.0073$ ) compared to vehicle. To maintain BBB integrity, adequate structural support from tight-junction (TJ) proteins is essential. We therefore quantified the expression levels of mRNAs encoding the TJ proteins claudin-5, ZO-1, and ZO-2 by qPCR at 24 h post-CCI. mRNA expression levels of claudin-5 (+40%) and ZO-1 (+60%) were significantly higher in the LD RNase1 group (+60%) compared to vehicle-treated animals. ZO-2 mRNA level was significantly higher in the MD- (+43%) and HD-RNase1 (+38%) groups compared to vehicle-treated animals, whereas ZO-2 mRNA expression was not increased by LD-RNase1 treatment (Fig. 3C–E).

## Discussion

This is the first study demonstrating that RNase1 injection can preserve the blood–brain barrier integrity in the early period following TBI. Low-dose RNase1 upregulated multiple TJ protein mRNA levels, and reduced edema, inflammatory cell infiltration, macrophage activation and lesion volume. However, the treatment protocol (2 doses, at 30 min and 12 h post-contusion) was not sufficient for long-term reduction in lesion size, suggesting that pretreatment or prolonged post-treatment may be necessary. For instance, a protective effect against post-operative dementia and brain edema after stroke could only be achieved with RNase1 pretreatment<sup>22,31</sup>.

**Effects on brain edema.** Vasogenic edema and IgG extravasation were reduced at one day post-TBI. The pathogenic effect of cfRNA may be partially attributed to reduced ZO-1 and claudin-5 expression<sup>33</sup>, while RNase1 can increase expression of ZO-1, ZO-2, and claudin-5, suggesting a stabilizing effect on BBB integ-

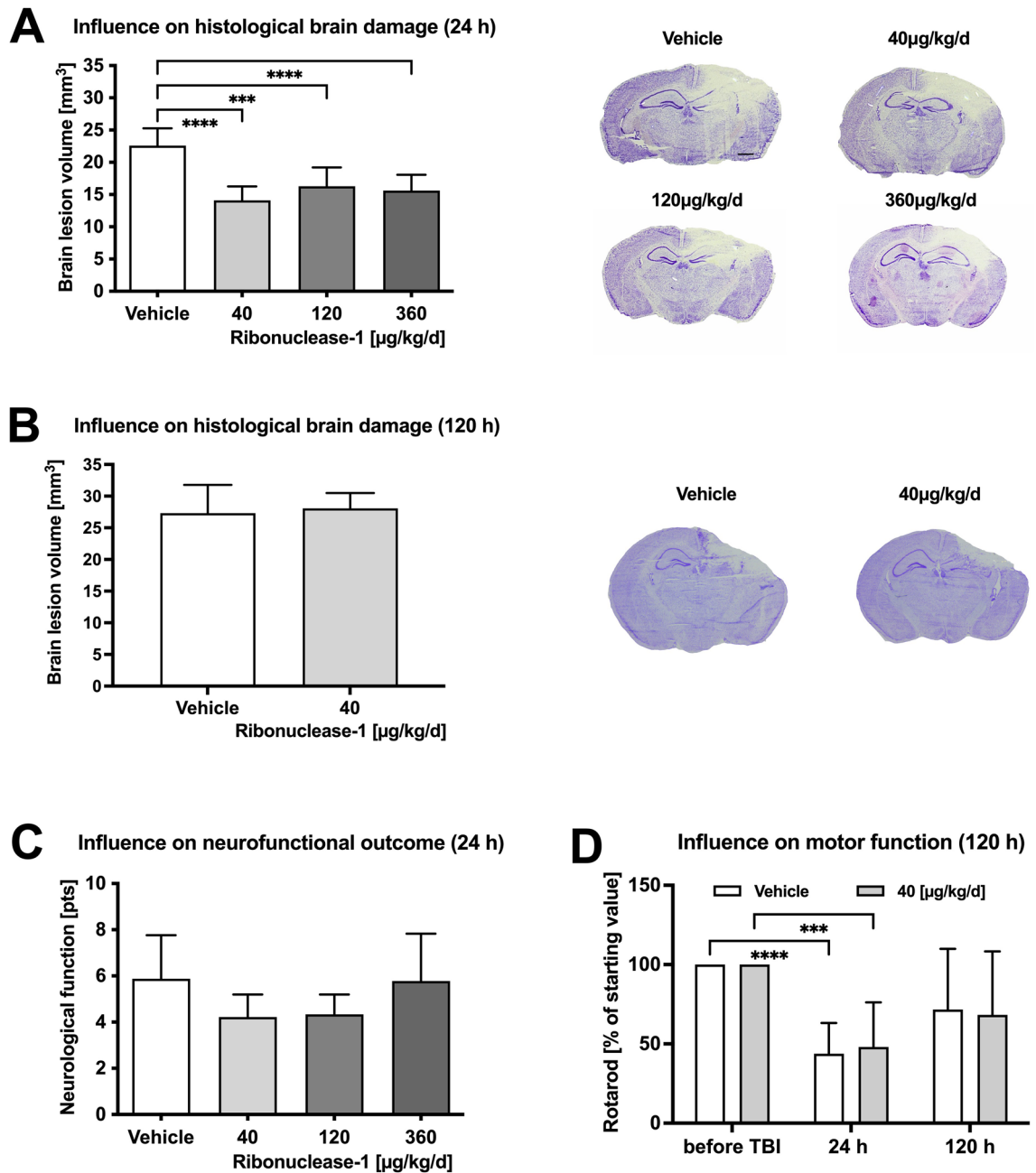


**Figure 1.** Influence on brain lesion and functional outcome. Brain lesion was determined 24 h (A) after controlled cortical impact injury in animals treated with RNase1 40, 120, 360 µg/kg/d or vehicle-solution (NaCl 0.9%, n = 10 each) by intraperitoneal injection 30 min and 12 h after brain insult. Treatment significantly reduced brain lesion volume in all treatment groups. With equal regime and amount of RNase1 120 h after CCI (B) impact lesion volume revealed no persistent treatment success. Neurofunctional deficits were determined at 24 h (C) and showed no effects on outcome with low dose showing the best score but failing to reach level of significance. The motoric function (D) was severely affected after 24 h, and animals recovered mainly after 120 h without significant difference between treatment and vehicle (n = 10/group). Data are presented as mean ± standard deviation; P values are adjusted for multiple comparisons by Sidak correction. The figure was generated with GraphPad Prism 9.0.

ity. Under cerebral ischemia, vascular permeability is increased by cfrNA via the VEGF axis<sup>6</sup>. TBI leads to an upregulation<sup>34</sup> or downregulation<sup>35</sup> of VEGF and would be a possible candidate for more detailed analyses in future studies.

**Anti-inflammatory effects.** In addition to VEGF signaling, cfrNAs stimulate the immune system via TLRs<sup>11,12,18,36</sup>, which induces the release of pro-inflammatory cytokines<sup>10</sup> and shifts microglial phenotype to the pro-inflammatory M1 type<sup>37,38</sup> known to induce neuronal damage and CNS dysfunction<sup>39</sup>. However, these anti-

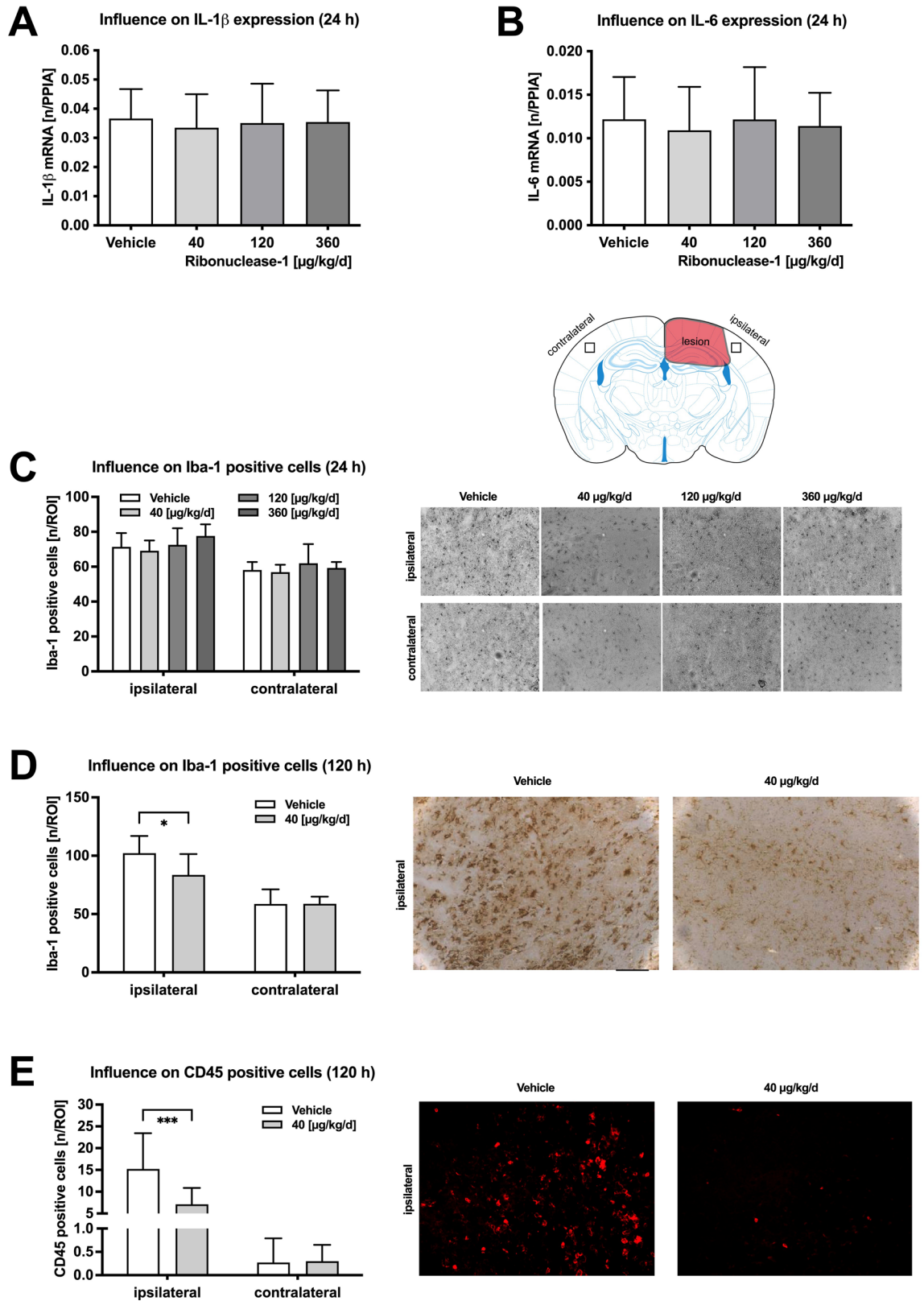


**Figure 2.** Regulation of markers for inflammation. Expression of inflammatory marker genes IL-1  $\beta$  (A) and IL-6 (B) were quantified and showed no treatment dependent effect. As marker for microglia activation the number of Iba-1 positive cells (C) were quantified and showed no difference between treatment (n = 10 each) groups 24 h after CCI. Iba-1 positive cells were quantified at 24 h and 120 h, and CD45-positive cells at 120 h after trauma using the same standardized region of interest as shown in the overview image (C). Contralateral number of Iba-1 positive cells remained identical 120 h after trauma (C). Pericontusional increase of Iba1- cells was significantly lower in the RNase1 treated mice (D) linked to a significant decrease of CD45 positive cells (E) in the RNase group (n = 10/group) 120 h after CCI. Data are presented as mean  $\pm$  standard deviation; P values are adjusted for multiple comparisons by Sidak correction. The figure was generated with GraphPad Prism 9.0.

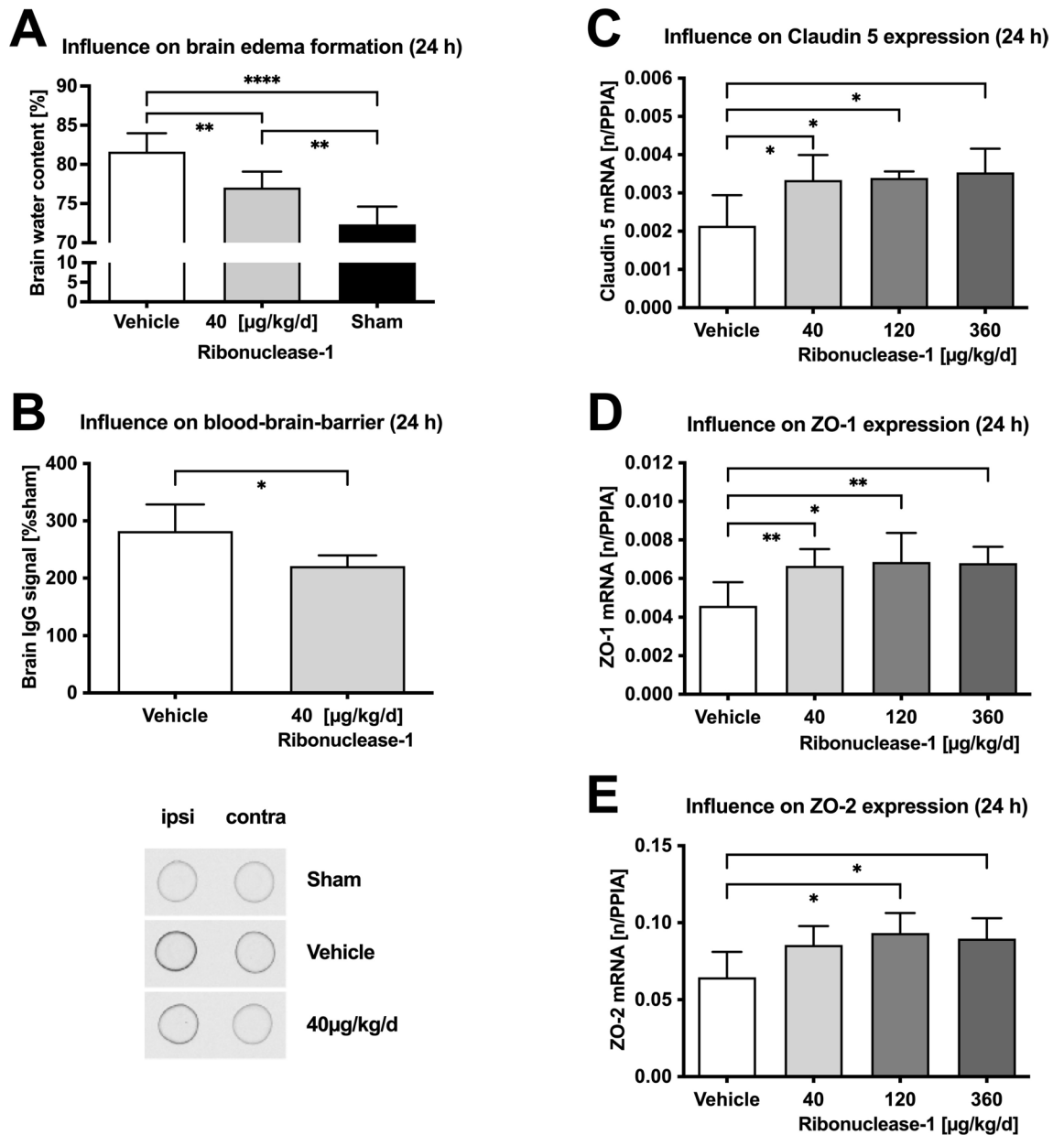


**Figure 3.** Influence on cerebral edema and regulation of tight junction protein mRNAs. Brain water content determined 24 h after CCI (A) was significantly lower with 40 µg/kg/d RNase1 compared to vehicle solution (n = 10 each). Integrity of the blood-brain barrier was investigated 24 h after lesion by quantification of immunoglobulin G (IgG) extravasation (B), which was significantly lower in RNase treated animals (n = 10 each). 24 h after insult mRNA expression of claudin 5 (C), ZO-1 (D), and ZO-2 (E) was quantified to investigate the impact of RNase treatment on VEGF regulated tight junction protein and showed significantly higher values with RNase treatment (n = 10 each). Data are presented as mean ± standard deviation; P values are adjusted for multiple comparisons by Sidak correction. The figure was generated with GraphPad Prism 9.0.

inflammatory actions appear to play only a minor role in the first 24 h post-CCI as there no alterations in IL-6 and IL-1β mRNA expression or microglial number, while significantly reduced numbers of Iba1 + and CD45 + cells were found at 120 h post-CCI. Due to the early beneficial effects on the BBB and immune system<sup>10–19</sup>, reduced neuroinflammation was still detected 120 h post-TBI. Collectively, these findings suggest that cRNAs released during TBI induce leukocyte extravasation via VEGF2 activation<sup>10</sup> and a simultaneous shift to the pro-inflammatory M1-phenotype<sup>15</sup>.

At 5 days after injury, brain lesion volume was similar between groups, suggesting that the initial putative beneficial effect was not long-lasting and not sufficient to result in functional improvement.

**Limitations of the study.** These findings suggest that RNase1 treatment may be a useful adjunct therapy to reduce or delay secondary damage in the early phase post-TBI. Indeed, high cRNA in systemic circulation is



associated with poor outcome after TBI<sup>23,40</sup>. Further, RNase1 released from endothelial cells during ischemia<sup>28,41</sup> may serve an endogenous protective function<sup>42</sup>. Thus, RNase1 treatment supplements an endogenous mechanism. RNase1 degrades ssRNAs but not extracellular rRNAs, mRNAs, or miRNAs. In a mouse model of myocardial infarction, RNase1 treatment reduced myocardial edema and infarct size<sup>42,43</sup>. While this presumably reflects degradation of cfRNA, it is currently challenging to directly measure cfRNAs in small volumes of mouse plasma<sup>31,43,44</sup>. However, these protective effects of RNase1 treatment after TBI are consistent with suppression of pathways known to be activated by cfRNAs. RNase1 attenuated septic cardiomyopathy and cardiac apoptosis in a murine model of polymicrobial sepsis. Whereas there was no clear evidence of reduction in cfRNA nor a correlation between RNase1 and cfRNA levels<sup>44</sup>. After myocardial infarction in mice systemic application of RNase1 reduced edema formation and infarct size and improved survival. Plasma cfRNA levels were significantly increased compared with controls at 30 min after ligation, but no difference were present between treatment groups<sup>43</sup>. Exosomes<sup>45</sup>, microRNA<sup>46</sup>, or long non-coding RNA<sup>47</sup> could possibly serve as indirect markers for cfRNA. Especially in *in vivo* studies with small rodents to overcome the limitation of limited plasma sample size.

Despite clear data on brain edema formation and early histological brain damage, the present study fails to provide evidence for functional improvement by RNase1 therapy after experimental TBI. Although the RNase1-treated animals have lower mean scores in the neuro-deficit score 24 h after CCI, these changes were not significant. Rotarod data failed to show any effect at 24 h and 5 days after injury. Reduction in extent of brain edema, blood–brain-barrier disruption and brain lesion at 24 h post injury therefore does not result in improved functional recovery. Furthermore, brain water levels were lower than expected and compared to recent other studies. Although the vacuum method is superior to the conventional oven technique in terms of quantifying water content in small samples<sup>48</sup>, the low water levels in all samples suggest a systemic measurement bias, which was equally evident in all experimental groups. Therefore, we decided to present the ipsi- and contralateral data to demonstrate the relative changes induced by RNase1 treatment.

In addition, only male animals are used in the study. We therefore cannot estimate the gender effect and the impact of RNase1 treatment in brain injured female mice. These effects need to be addressed in future studies.

To reduce the number of animals the study focused on the effect of RNase1 in brain injured animals. Therefore, the influence of RNase1 in sham or healthy animals was not investigated in detail. Only in the study groups to determine brain-water content RNase1 was also given to sham animals. In these animals, neurological function was not negatively influenced by RNase1 and were all 0 = normal (Figure S1). This indicates that RNase1 treatment does not have a highly negative impact on neurological function. Future studies should address in more detail the effect in sham or naïve animals to rule out any negative influence of RNase1.

## Conclusion

We demonstrate that *i.p.* RNase1 can stabilize the BBB following TBI, resulting in reduced vasogenic edema, leukocyte recruitment, and microglial activation in perilesional tissue. These data support a role for cfRNA and RNase1 in pathophysiology of TBI.

## Materials and methods

**Animals.** This study was approved by the German animal protection committee (Landesuntersuchungsamt Rheinland-Pfalz, protocol number G-13-1-074). Experiments were performed in accordance with all national animal welfare guidelines and ARRIVE guidelines for reporting animal research<sup>49</sup>. The study was conducted using 90 male C57Bl6/N mice (Charles River Laboratories, Sulzfeld, Germany; weight: 22–28 g). Due to signs of severe stress, one animal in each of the two treatment arms (120 h survival time) was euthanized prior to the end of the observation period to prevent unnecessary suffering. The study protocol did not allow replacement of excluded animals.

**Drug preparation.** Ribonuclease-1 (RNase1, Sigma, Germany) was dissolved in sterile normal saline by a third person not involved in the experiments or analysis, numbered and prepared for intraperitoneal (*i.p.*) injection. The experiments and the processing of the material was performed in blinded fashion. The syringes were covered to prevent identification of the solution and to ensure blinding of the person performing the injection. Mice were randomly allocated to receive two *i.p.* injections of 20, 60, or 180 µg/kg RNase1 or vehicle at 30 min and 12 h post-TBI. These doses are at least tenfold lower than required to induce adverse side effects in rodents<sup>6,22,31</sup>. To minimize the total number of animals used in accordance with ARRIVE guidelines<sup>49</sup>, no additional sham group was established for most experiments. Also, after the initial dose–response study, subsequent investigations of brain water accumulation, tissue IgG changes, and 120-h survival used only the most effective (low) dose of RNase1, with sham animals examined for comparison only when necessary. Sham animals received either LD-RNase1 solution.

**Traumatic brain injury.** Traumatic brain injury was induced by CCI using an electromagnetic impact device (Leica Impact One™ Stereotaxic Impactor, Richmond, IL; tip: 3 mm; velocity: 6 m/s; duration: 200 ms; displacement: 1.5 mm). The settings were chosen to induce severe brain injury. Animals were anesthetized by intraperitoneal injection of 5 mg/kg midazolam, 0.05 mg/kg fentanyl, and 0.5 mg/kg medetomidine, an air/oxygen mixture (40% O<sub>2</sub>) was supplied via facemask in spontaneously breathing animals and body temperature was maintained at 37 °C rectal temperature with a feedback-controlled heating pad (Hugo Sachs, March-Hugstetten, Germany). Animals were fixed in a stereotactic frame (Kopf Instruments, Tujunga, USA) and a craniotomy (4 × 4 mm) was performed using a saline-cooled high-speed drill above the right parietal cortex between the sagittal, lambdoid, and coronal sutures and the insertion of the temporal muscle. Trauma was induced perpendicular and directly to right cortex by an experimenter blinded to treatment group allocation<sup>50–52</sup>. Thereafter,

the craniotomy was closed with the initially removed bone, fixed with tissue glue (Histoacryl, Braun-Melsungen, Melsungen, Germany), the wound was closed with filament sutures and anesthesia was antagonized using 0.5 mg/kg Flumazenil and 2.5 mg/kg Atepeamezol hydrochloride. Animals were allowed to recover for 1.5 h in a neonatal incubator (IC8000, Draeger, Luebeck, Germany) with controlled air temperature (35 °C) and ambient humidity (35%).

**Neurological outcome and Rotarod test.** Before CCI (1 h) and at 24 h after CCI, an investigator blinded to experimental group assigned a neurologic severity score ranging from 0 (healthy) to 15 (severely impaired) (24 h groups: N=40)<sup>53</sup>. An accelerating rotarod test (Rotarod Treadmill, MED Associates, INC, St Albans, VT) was conducted in the long-time surviving groups one day before and at 24 and 120 h post-CCI (N=20). The rotarod speed was increased linearly from 4 to 40 rpm over 5 min. The investigation was completed when the mice fell off the rods. Briefly, each mouse was placed on an accelerating rotating cylinder, and the time and maximum speed at which the animal fell off (27 cm fall height) were recorded<sup>54,55</sup>. Four rotarod tasks were conducted before CCI and the mean value of each animal was defined as 100% “starting value”. 24 h and 120 h following injury, animals were tested in two trials per time point, averaged and evaluated relative to pre-injury latencies to correct for individual pre-injury performance.

**Tissue preparation, Nissl, Iba-1 and CD45 staining.** Animals were deeply anesthetized by intraperitoneal injection of 5 mg/kg midazolam, 0.05 mg/kg fentanyl, and 0.5 mg/kg medetomidine. After cervical dislocation and decapitated, the brains were carefully excised, frozen in powdered dry ice, and stored at -20 °C. Coronal Sects. (10 µm) were cut at 500 µm intervals (24 h: n=40 mice, 120 h: n=20 mice), collected on Superfrost Plus Slides (Thermo Fisher, Waltham, MA, USA) and subjected to cresyl violet staining. The first section was taken at bregma + 3.14 mm according to the Mouse Brain Library atlas (<http://www.mbl.org>). Brain lesion volume was measured using a computerized image system (DeltaPix InSight, Smorum, Denmark)<sup>56</sup>. In brief, to control for the effect of brain edema, the area of uninjured brain tissue and the total area of the contralateral hemisphere were quantified in each section. Afterwards the injured area was calculated by subtraction of “normal” area in the injured hemisphere from total contralateral. Other slices were immunostained for the activated microglial marker Iba-1 using an anti-rabbit Iba-1 antibody (1:1500, Wako Pure Chemical Industries, Osaka, Japan) and a biotinylated anti-rabbit IgG (Vector Laboratories Inc., Burlingame, CA). Signals were detected using ABC Complex (Vector) and DAB (Thermo-Fischer, Waltham, MA). The appearance of Iba-1+/CD45+ cells 120 h after lesion induction was quantified by dual staining using rat anti-CD45 (1:500, Thermo-Fisher) with Alexa Fluor 568-conjugated goat anti-rat IgG (1:500, Thermo-Fisher, Waltham, MA) and anti-rabbit Iba-1 antibody (1:500, Wako) with Alexa Fluor 488-conjugated goat anti-rabbit IgG (1:500, Thermo-Fisher). Sections were then counterstained with DAPI (1:10,000, Thermo-Fisher)<sup>57</sup>. Images were acquired at 20× magnification, and cells were counted in the perilesional and corresponding, non-injured contralateral regions of two serial sections in the zone with the largest lesion (bregma -1.64 mm and bregma -1.82 mm, [www.mbl.org](http://www.mbl.org), ROI: 2.55 mm<sup>2</sup>)<sup>55</sup>. In the predefined areas (border zone at lower outside corner the lesion and the corresponding contralateral side) double-immunolabeled cells were counted by an investigator blinded to treatment using ImageJ (U.S. National Institutes of Health, Bethesda, MD).

**RNA isolation and quantitative polymerase chain reaction (qPCR).** For mRNA analysis brain tissue samples were taken from the trimming slices. The right upper quadrant (lesioned brain tissue) of coronal trimming sections were collected (n=40) as previously described<sup>52</sup>, frozen in liquid nitrogen, and stored at -80 °C<sup>58</sup>. RNA extraction, reverse transcription, and mRNA quantification by real-time RT-PCR were performed as described<sup>53,56</sup>. Absolute copy numbers of target genes were normalized to the reference gene cyclophilin A (*PPIA*).

**Brain water content.** Brains were removed 24 h after trauma and placed in a mouse brain matrix. Brains were cut half along the interhemispheric plane and 6 mm slides was taken containing the lesion or the corresponding contralateral side (n=30), weighed (wet weight, WW), dried in a vacuum-centrifuge (Univapo 100H, UniEquip, Planegg, Germany) for 48 h, and reweighed (dry weight, DW). Brain water content was calculated according to the equation water content (%) = (WW - DW) / WW × 100<sup>48</sup>.

**IgG quantification.** The dry-frozen tissue samples (after vacuum-drying to determine the brain water content) were stored at -80 °C. Samples were lysed in RIPA buffer (n=30), and total cellular proteins separated by SDS-PAGE, transferred to nitrocellulose membranes, immunolabeled (IgG; 1:10 000; Li-cor), and visualized by a near-infrared laser scanning system (LI-COR Odyssey) essentially as described<sup>58</sup>. An antibody against GAPDH (Acris, clone 6C5) was used as the reference and quantification was performed using ImageJ (NIH, MD).

**Statistics.** All experiments were randomized and performed by blinded investigators (computer-based randomization). The experimental groups are presented in Fig. 4. To determine the required sample size, an a priori power analysis was performed using G\*Power<sup>59</sup> based on lesion volume data from previous studies. A priori power analysis for an effect size of 0.7 suggested that a standard statistical power (1-β) of Pβ=0.95 and significance level (α) of 0.05 can be obtained for expected lesion volumes using 10 subjects per group (4 groups) and for expected brain water content using 10 subjects per group (2 groups). GraphPad Prism 9 statistical software (GraphPad Software Inc., La Jolla, CA, USA) was used to perform statistical analysis. Prior to analysis, we checked the test assumptions. Due to the limited power in small samples, we did not perform formal

# Study Design

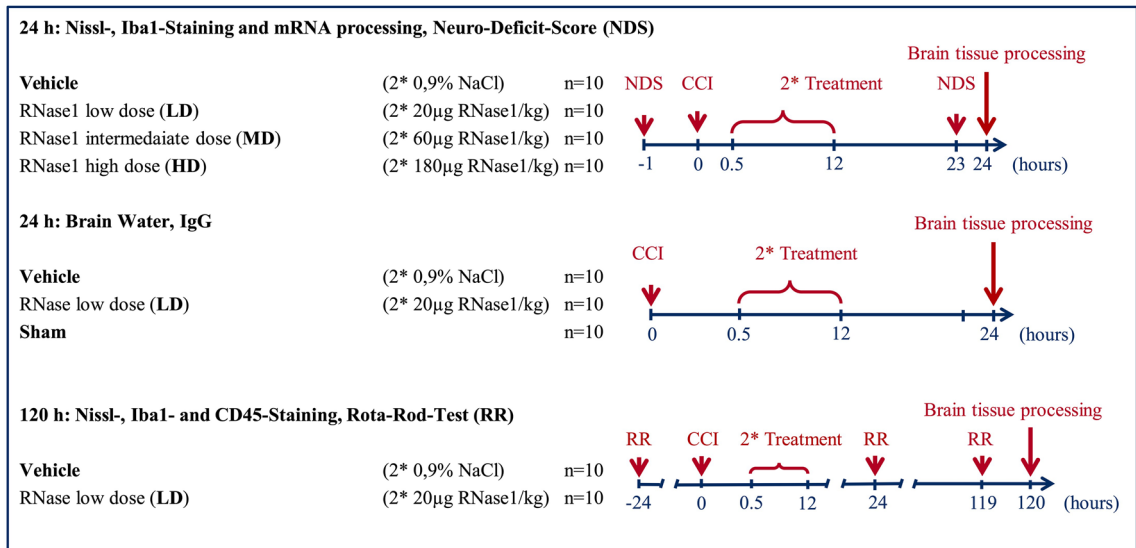


**Figure 4.** Study Design. The study was performed with 90 male mice. Only the most effective (low) dose of RNase1 was used for subsequent studies of brain water accumulation, tissue IgG changes, and 120-h survival. The figure was generated with Microsoft PowerPoint.

goodness-of-fit tests prior to the t test or ANOVA, but instead relied on the graphical assessment of distribution characteristics<sup>60</sup>. Normality was checked by inspecting the unimodality and symmetry of histograms, as well as by Q-Q plots. The equality of variances was checked by inspecting histograms and standard deviations. For comparison of multiple independent groups, Brown-Forsythe and Welch ANOVA with post-hoc Dunnett T3 multiple comparisons test (comparisons between all groups) was employed. To evaluate group differences in repeated measurements from the same animals (rotarod), RM two-way ANOVA was applied (factors: treatment and time), followed by Šidák's multiple comparisons test. Comparisons between two independent groups were carried out by the Welch's t test. Values of  $p < 0.05$  were considered significant. Data are presented as the mean and standard deviation (mean  $\pm$  SD).

## Data sharing

All datasets generated and analyzed during this study are kept in the Dept. of Anesthesiology, Medical Center of the Johannes Gutenberg-University and are available from the corresponding author upon reasonable request.

Received: 5 October 2021; Accepted: 22 March 2022

Published online: 06 April 2022

## References

- Pan, Y. B., Sun, Z. L. & Feng, D. F. The role of MicroRNA in traumatic brain injury. *Neuroscience* **367**, 189–199. <https://doi.org/10.1016/j.neuroscience.2017.10.046> (2017).
- Vourc'h, M., Roquilly, A. & Asehnoune, K. Trauma-induced damage-associated molecular patterns-mediated remote organ injury and immunosuppression in the acutely ill patient. *Front. Immunol.* **9**, 1330. <https://doi.org/10.3389/fimmu.2018.01330> (2018).
- Szilágyi, M. *et al.* Circulating cell-free nucleic acids: Main characteristics and clinical application. *Int. J. Mol. Sci.* **21**, 1. <https://doi.org/10.3390/ijms21186827> (2020).
- Diehl, F. *et al.* Detection and quantification of mutations in the plasma of patients with colorectal tumors. *Proc. Natl. Acad. Sci. USA* **102**, 16368–16373. <https://doi.org/10.1073/pnas.0507904102> (2005).
- Contreras-Naranjo, J. C., Wu, H. J. & Ugaz, V. M. Microfluidics for exosome isolation and analysis: Enabling liquid biopsy for personalized medicine. *Lab. Chip* **17**, 3558–3577. <https://doi.org/10.1039/c7lc00592j> (2017).
- Fischer, S. *et al.* Extracellular RNA mediates endothelial-cell permeability via vascular endothelial growth factor. *Blood* **110**, 2457–2465. <https://doi.org/10.1182/blood-2006-08-040691> (2007).
- Werner, C. & Engelhard, K. Pathophysiology of traumatic brain injury. *Br. J. Anaesth.* **99**, 4–9. <https://doi.org/10.1093/bja/aem131> (2007).
- Thal, S. C. & Neuhaus, W. The blood-brain barrier as a target in traumatic brain injury treatment. *Arch. Med. Res.* **45**, 698–710. <https://doi.org/10.1016/j.arcmed.2014.11.006> (2014).
- Toffolo, K. *et al.* Circulating microRNAs as biomarkers in traumatic brain injury. *Neuropharmacology* **145**, 199–208. <https://doi.org/10.1016/j.neuropharm.2018.08.028> (2019).
- Fischer, S. *et al.* Extracellular RNA promotes leukocyte recruitment in the vascular system by mobilising proinflammatory cytokines. *Thromb. Haemost.* **108**, 730–741. <https://doi.org/10.1160/TH12-03-0186> (2012).
- Bertheloot, D. *et al.* RAGE enhances TLR responses through binding and internalization of RNA. *J. Immunol.* **197**, 4118–4126. <https://doi.org/10.4049/jimmunol.1502169> (2016).



12. Gantier, M. P. *et al.* TLR7 is involved in sequence-specific sensing of single-stranded RNAs in human macrophages. *J. Immunol.* **180**, 2117–2124. <https://doi.org/10.4049/jimmunol.180.4.2117> (2008).
13. Noll, F. *et al.* Self-extracellular RNA acts in synergy with exogenous danger signals to promote inflammation. *PLoS ONE* **12**, e0190002. <https://doi.org/10.1371/journal.pone.0190002> (2017).
14. Alexopoulou, L., Holt, A. C., Medzhitov, R. & Flavell, R. A. Recognition of double-stranded RNA and activation of NF-kappaB by Toll-like receptor 3. *Nature* **413**, 732–738. <https://doi.org/10.1038/35099560> (2001).
15. Melton, L. M. *et al.* Chronic glial activation, neurodegeneration, and APP immunoreactive deposits following acute administration of double-stranded RNA. *Glia* **44**, 1–12. <https://doi.org/10.1002/glia.10276> (2003).
16. Jensen, M. B., Hegelund, I. V., Lomholt, N. D., Finsen, B. & Owens, T. IFNgamma enhances microglial reactions to hippocampal axonal degeneration. *J. Neurosci.* **20**, 3612–3621 (2000).
17. Zhang, L. J. *et al.* Antimicrobial peptide LL37 and MAVS signaling drive interferon-beta production by epidermal keratinocytes during skin injury. *Immunity* **45**, 119–130. <https://doi.org/10.1016/j.immuni.2016.06.021> (2016).
18. Chen, C. *et al.* Role of extracellular RNA and TLR3-Trif signaling in myocardial ischemia-reperfusion injury. *J. Am. Heart Assoc.* **3**, e000683. <https://doi.org/10.1161/jaha.113.000683> (2014).
19. Kim, H. *et al.* Double-stranded RNA mediates interferon regulatory factor 3 activation and interleukin-6 production by engaging Toll-like receptor 3 in human brain astrocytes. *Immunology* **124**, 480–488. <https://doi.org/10.1111/j.1365-2567.2007.02799.x> (2008).
20. Begemann, M., Leon, M., van der Horn, H. J., van der Naalt, J. & Sommer, I. Drugs with anti-inflammatory effects to improve outcome of traumatic brain injury: A meta-analysis. *Sci. Rep.* **10**, 16179. <https://doi.org/10.1038/s41598-020-73227-5> (2020).
21. Tang, H. *et al.* Progesterone and vitamin D: Improvement after traumatic brain injury in middle-aged rats. *Horm. Behav.* **64**, 527–538. <https://doi.org/10.1016/j.yhbeh.2013.06.009> (2013).
22. Walberer, M. *et al.* RNase therapy assessed by magnetic resonance imaging reduces cerebral edema and infarction size in acute stroke. *Curr. Neurovasc. Res.* **6**, 12–19 (2009).
23. Macher, H. *et al.* Role of early cell-free DNA levels decrease as a predictive marker of fatal outcome after severe traumatic brain injury. *Clin. Chim. Acta* **414**, 12–17. <https://doi.org/10.1016/j.cca.2012.08.001> (2012).
24. Futami, J. *et al.* Tissue-specific expression of pancreatic-type RNases and RNase inhibitor in humans. *DNA Cell Biol.* **16**, 413–419. <https://doi.org/10.1089/dna.1997.16.413> (1997).
25. Morita, T., Niwata, Y., Ohgi, K., Ogawa, M. & Irie, M. Distribution of two urinary ribonuclease-like enzymes in human organs and body fluids. *J. Biochem.* **99**, 17–25 (1986).
26. Yasuda, T., Nadano, D., Takeshita, H. & Kishi, K. Two distinct secretory ribonucleases from human cerebrum: purification, characterization and relationships to other ribonucleases. *Biochem. J.* **296**(Pt 3), 617–625 (1993).
27. Barrabes, S. *et al.* Glycosylation of serum ribonuclease 1 indicates a major endothelial origin and reveals an increase in core fucosylation in pancreatic cancer. *Glycobiology* **17**, 388–400. <https://doi.org/10.1093/glycob/cwm002> (2007).
28. Landre, J. B. *et al.* Human endothelial cells selectively express large amounts of pancreatic-type ribonuclease (RNase 1). *J. Cell Biochem.* **86**, 540–552. <https://doi.org/10.1002/jcb.10234> (2002).
29. Timaru-Kast, R. *et al.* Delayed inhibition of angiotensin II receptor type 1 reduces secondary brain damage and improves functional recovery after experimental brain trauma\*. *Crit. Care Med.* **40**, 935–944. <https://doi.org/10.1097/CCM.0b013e31822f08b9> (2012).
30. Thal, S. C. *et al.* Pioglitazone reduces secondary brain damage after experimental brain trauma by PPAR-gamma-independent mechanisms. *J. Neurotrauma* **28**, 983–993. <https://doi.org/10.1089/neu.2010.1685> (2011).
31. Chen, C. *et al.* Protective effect of RNase on unilateral nephrectomy-induced postoperative cognitive dysfunction in aged mice. *PLoS ONE* **10**, e0134307. <https://doi.org/10.1371/journal.pone.0134307> (2015).
32. Hummel, R. *et al.* Single intracerebroventricular progesterone injection adversely affects the blood-brain barrier in experimental traumatic brain injury. *J. Neurochem.* **158**, 342–357. <https://doi.org/10.1111/jnc.15375> (2021).
33. Thal, S. C. *et al.* Volatile anesthetics influence blood-brain barrier integrity by modulation of tight junction protein expression in traumatic brain injury. *PLoS ONE* **7**, e50752. <https://doi.org/10.1371/journal.pone.0050752> (2012).
34. Sköld, M. K., von Gertten, C., Sandberg-Nordqvist, A. C., Mathiesen, T. & Holmin, S. VEGF and VEGF receptor expression after experimental brain contusion in rat. *J. Neurotrauma* **22**, 353–367. <https://doi.org/10.1089/neu.2005.22.353> (2005).
35. Wright, D. K. *et al.* Behavioral, blood, and magnetic resonance imaging biomarkers of experimental mild traumatic brain injury. *Sci. Rep.* **6**, 28713. <https://doi.org/10.1038/srep28713> (2016).
36. Ganguly, D. *et al.* Self-RNA-antimicrobial peptide complexes activate human dendritic cells through TLR7 and TLR8. *J. Exp. Med.* **206**, 1983–1994. <https://doi.org/10.1084/jem.20090480> (2009).
37. Cabrera-Fuentes, H. A. *et al.* Regulation of monocyte/macrophage polarisation by extracellular RNA. *Thromb. Haemost.* **113**, 473–481. <https://doi.org/10.1160/TH14-06-0507> (2015).
38. Kumar, A. *et al.* Microglial-derived microparticles mediate neuroinflammation after traumatic brain injury. *J. Neuroinflamm.* **14**, 47. <https://doi.org/10.1186/s12974-017-0819-4> (2017).
39. Stoica, B. A. & Faden, A. I. Cell death mechanisms and modulation in traumatic brain injury. *Neurotherapeutics* **7**, 3–12. <https://doi.org/10.1016/j.nurt.2009.10.023> (2010).
40. Rodrigues Filho, E. M. *et al.* Elevated cell-free plasma DNA level as an independent predictor of mortality in patients with severe traumatic brain injury. *J. Neurotrauma* **31**, 1639–1646. <https://doi.org/10.1089/neu.2013.3178> (2014).
41. Sznajd, J., Magdon, M., Naskalski, J. W., Urcacz, R. & Wojcikiewicz, O. Serum ribonuclease activity in acute myocardial infarction. *Cor. Vasa* **23**, 241–247 (1981).
42. Cabrera-Fuentes, H. A. *et al.* RNase1 prevents the damaging interplay between extracellular RNA and tumour necrosis factor-alpha in cardiac ischaemia/reperfusion injury. *Thromb. Haemost.* **112**, 1110–1119. <https://doi.org/10.1160/th14-08-0703> (2014).
43. Stieger, P. *et al.* Targeting of extracellular RNA reduces edema formation and infarct size and improves survival after myocardial infarction in Mice. *J Am Heart Assoc* **6**, 1. <https://doi.org/10.1161/JAHA.116.004541> (2017).
44. Zechendorf, E. *et al.* Ribonuclease 1 attenuates septic cardiomyopathy and cardiac apoptosis in a murine model of polymicrobial sepsis. *JCI Insight* <https://doi.org/10.1172/jci.insight.131571> (2020).
45. Wang, P. *et al.* Plasma exosome-derived MicroRNAs as novel biomarkers of traumatic brain injury in rats. *Int. J. Med. Sci.* **17**, 437–448. <https://doi.org/10.7150/ijms.39667> (2020).
46. Atif, H. & Hicks, S. D. A review of MicroRNA biomarkers in traumatic brain injury. *J. Experim. Neurosci.* **13**, 1179069519832286. <https://doi.org/10.1177/1179069519832286> (2019).
47. Cuevas-Diaz Duran, R., Wei, H., Kim, D. H. & Wu, J. Q. Invited review: Long non-coding RNAs: Important regulators in the development, function and disorders of the central nervous system. *Neuropathol. Appl. Neurobiol.* **45**, 538–556. <https://doi.org/10.1111/nan.12541> (2019).
48. Sebastiani, A., Hirnet, T., Jahn-Eimermacher, A. & Thal, S. C. Comparison of speed-vacuum method and heat-drying method to measure brain water content of small brain samples. *J. Neurosci. Methods* **276**, 73–78. <https://doi.org/10.1016/j.jneumeth.2016.11.012> (2017).
49. Kilkenny, C., Browne, W. J., Cuthill, I. C., Emerson, M. & Altman, D. G. Improving bioscience research reporting: The ARRIVE guidelines for reporting animal research. *J. Pharmacol. Pharmacother.* **1**, 94–99. <https://doi.org/10.4103/0976-500x.72351> (2010).

50. Thal, S. C., Wyschkon, S., Pieter, D., Engelhard, K. & Werner, C. Selection of endogenous control genes for normalization of gene expression analysis after experimental brain trauma in mice. *J. Neurotrauma* **25**, 785–794. <https://doi.org/10.1089/neu.2007.0497> (2008).
51. Brody, D. L. *et al.* Electromagnetic controlled cortical impact device for precise, graded experimental traumatic brain injury. *J. Neurotrauma* **24**, 657–673. <https://doi.org/10.1089/neu.2006.0011> (2007).
52. Kramer, T. *et al.* Dimethyl fumarate treatment after traumatic brain injury prevents depletion of antioxidative brain glutathione and confers neuroprotection. *J. Neurochem.* **143**, 523–533. <https://doi.org/10.1111/jnc.14220> (2017).
53. Timaru-Kast, R. *et al.* Influence of age on brain edema formation, secondary brain damage and inflammatory response after brain trauma in mice. *PLoS ONE* **7**, e43829. <https://doi.org/10.1371/journal.pone.0043829> (2012).
54. Pottker, B. *et al.* Traumatic brain injury causes long-term behavioral changes related to region-specific increases of cerebral blood flow. *Brain Struct. Funct.* **222**, 4005–4021. <https://doi.org/10.1007/s00429-017-1452-9> (2017).
55. Kramer, T. J. *et al.* Depletion of regulatory T cells increases T cell brain infiltration, reactive astrogliosis, and interferon-gamma gene expression in acute experimental traumatic brain injury. *J. Neuroinflamm.* **16**, 163. <https://doi.org/10.1186/s12974-019-1550-0> (2019).
56. Sebastiani, A. *et al.* Proneurotrophin binding to P75 neurotrophin receptor (P75ntr) is essential for brain lesion formation and functional impairment after experimental traumatic brain injury. *J. Neurotrauma* **32**, 1599–1607. <https://doi.org/10.1089/neu.2014.3751> (2015).
57. Schaible, E. V. *et al.* 2-Methoxyestradiol confers neuroprotection and inhibits a maladaptive HIF-1 $\alpha$  response after traumatic brain injury in mice. *J. Neurochem.* **129**, 940–954. <https://doi.org/10.1111/jnc.12708> (2014).
58. Menzel, L. *et al.* Progranulin protects against exaggerated axonal injury and astrogliosis following traumatic brain injury. *Glia* **65**, 278–292. <https://doi.org/10.1002/glia.23091> (2017).
59. Faul, F., Erdfelder, E., Buchner, A. & Lang, A. G. Statistical power analyses using G\*Power 31: Tests for correlation and regression analyses. *Behav. Res. Methods* **41**, 1149–1160. <https://doi.org/10.3758/BRM.41.4.1149> (2009).
60. Schucany, W. R. & Tony Ng, H. K. Preliminary goodness-of-fit tests for normality do not validate the one-sample student t. *Commun. Stat. Theory Methods* **35**, 2275–2286. <https://doi.org/10.1080/03610920600853308> (2006).

## Acknowledgements

The authors thank Wieslawa Bobkiewicz, Tobias Hirnet, Frida Kornes, Dana Pieter, and Florian Pickart for their skilful assistance and critical validation during experimental investigations.

## Author contributions

T.K.: conception and design, experimental procedures, analysis, and interpretation of the results, writing the manuscript. P.H.: experimental procedures, analysis of the results. B.P., C.G., H.G., A.N., T.P.: analysis of the results, critical revision of the manuscript. K.R., M.S.: immunohistochemistry, interpretation of the results, critical revision of the manuscript. S.T.: conception and design, analysis, and interpretation of the results, writing the manuscript.

## Funding

Open Access funding enabled and organized by Projekt DEAL. This work was supported by institutional funding.

## Competing interests

The authors declare no competing interests.

## Additional information

**Supplementary Information** The online version contains supplementary material available at <https://doi.org/10.1038/s41598-022-09326-2>.

**Correspondence** and requests for materials should be addressed to S.C.T.

**Reprints and permissions information** is available at [www.nature.com/reprints](http://www.nature.com/reprints).

**Publisher's note** Springer Nature remains neutral with regard to jurisdictional claims in published maps and institutional affiliations.



**Open Access** This article is licensed under a Creative Commons Attribution 4.0 International License, which permits use, sharing, adaptation, distribution and reproduction in any medium or format, as long as you give appropriate credit to the original author(s) and the source, provide a link to the Creative Commons licence, and indicate if changes were made. The images or other third party material in this article are included in the article's Creative Commons licence, unless indicated otherwise in a credit line to the material. If material is not included in the article's Creative Commons licence and your intended use is not permitted by statutory regulation or exceeds the permitted use, you will need to obtain permission directly from the copyright holder. To view a copy of this licence, visit <http://creativecommons.org/licenses/by/4.0/>.

© The Author(s) 2022